L11 NEMS

Lecture notes by Ethan Minot, visiting from Oregon State University
ethan.minot@aalto.fi
Nanoelectronics Class at Aalto University, Autumn, 2021.

Lecture notes use material from:
Sorin's course notes from 2020
"The Physics of Nanoelectronics" Chapter 11 (Heikkila)
"Quantum Optomechanics" (Bowen & Milburn)

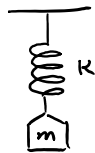PART 1   Monitoring the resonant freq of a small oscillators

- Force sensing
- Mass sensing

PART 2   Measurement & minipulation of macroscopic resonators
at their quantum limit.

APPENDIX   Details about applying input-output formalism
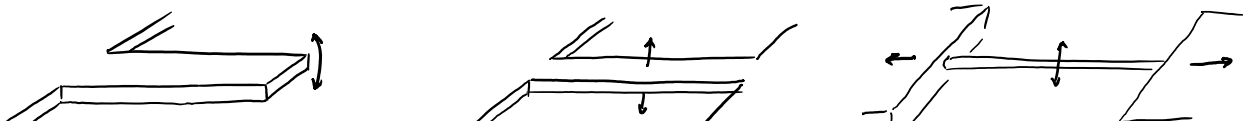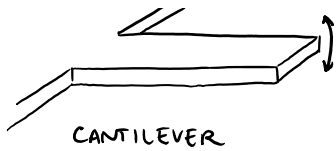and RWA to optomechanical systems.

PART 1

Monitoring resonant freq

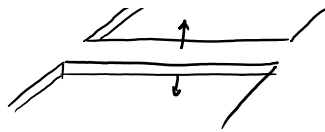$$\omega_0 = \sqrt{\frac{K}{m}}$$

Any change in K or m shows up in a measurement of ω_0

→ useful applications in nanoscience

Common resonator geometries that can be engineered from materials like
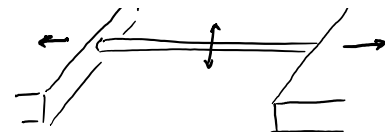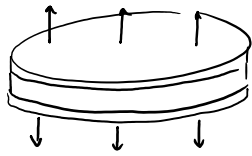silicon, quartz, aluminium, graphene, carbon nanotubes...

CANTILEVER

BEAM

"STRING" UNDER TENSION

DILATATION OSCILLATOR
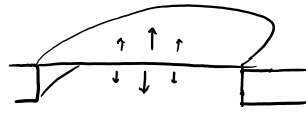
DRUM HEAD
(cross-sectional view)

For a given resonator geometry we can model the nth vibrational mode using $m_{eff,n}$ & $k_{eff,n}$
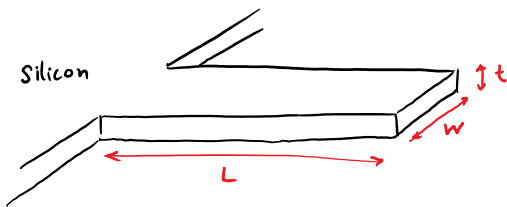
Silicon

$$K_{eff,1} = \frac{Ew}{4}\left(\frac{t}{L}\right)^3$$

~100 GPa

$$m_{eff,1} \approx \frac{1}{2}\rho Lwt$$

~2000 $\frac{kg}{m^3}$
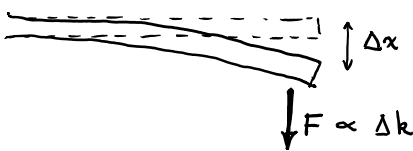
Hookes law approximation

$$F = K_{eff}\,\Delta x$$

$F \propto \Delta k$

Δx

Young's modulus examples
Silicon $E = 140$ GPa
Aluminum $E = 70$

Example 1:   For atomic force microscopy,

I want $K_{eff} \approx \dfrac{10nN}{1nm}$ because this is the typical "spring" holding solids together. I want $\omega_1 \approx 2\pi\,[200\,kHz]$ so I can make fast measurements.

I want L & w big enough to reflect a laser spot.

Possible dimensions: $L = 150 \mu m$
$w = 30 \mu m$
$t = 3 \mu m$

Example 2: I want resonant freq of an oscillator to change
by a measurable amount when one
atom lands on the oscillator.

For this application, must consider quality factor, Q.

Position
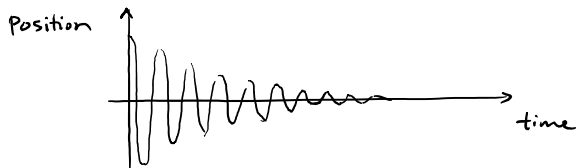
Q = Number of oscillations during ring down

$\frac{1}{Q}$ = fraction of energy lost per cycle.

Q determines how precisely we can measure ω_1

Fourier transform of the ring down

$\frac{\omega_1}{Q}$

ω_1 ω
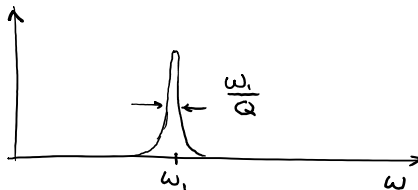
(Same result if you sweep driving freq and monitor amplitude)

Added mass, Δm causes $\Delta \omega_1$

$\Delta \omega_1 = \frac{\partial \omega_1}{\partial m} \Delta m$ $\omega = K_{eff}^{1/2} \, m_{eff}^{-1/2}$

$= -\frac{\Delta m}{2 m_{...}} \omega_1$

$$o m$$

$$= -\frac{\Delta m}{2 m_{eff}} \omega_1$$

Require $\quad \Delta\omega \gtrsim \frac{\omega_1}{Q}$

i.e. $\quad \frac{\Delta m}{2 m_{eff}} \gtrsim \frac{1}{Q}$

If we can get $Q \approx 10^5$, we need $m_{eff} \approx 10^5$ atoms

and we need a way to actuate/monitor ω.

One such oscillator is a carbon nanotube under tension

Chaste et al. "A nanomechanical mass sensor with yoctogram resolution" Nature Nanotechnology (2012)

$1\mu m$ length $\Rightarrow m_{eff} \approx 100,000\ m_{carbon}$
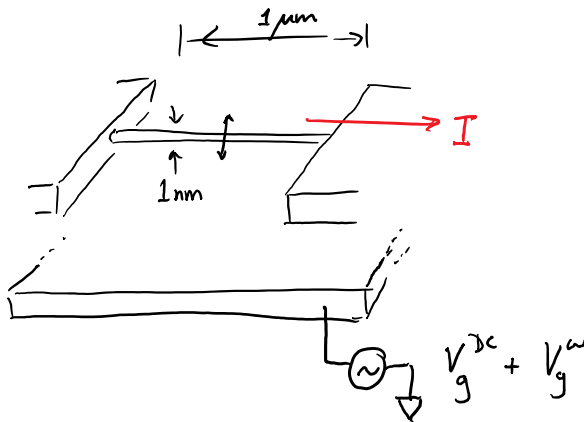
Clever way to actuate & measure

Conductance modulated by the total charge in conduction band

$$G = \frac{dG}{dq} q$$

q depends on ...

$$q = \tilde{C}_g(\omega) V_g^{DC}$$

$$= \frac{dC_g}{dz} z(\omega) V_g^{DC}$$

$$G = G_{DC} + \tilde{G} \cos \omega t$$

oscillation of G caused by motion of oscillator

Current through the channel

$$I = G V_{sd}$$

Modulate V_{sd} at a different freq, ω'

$$V_{sd} = \tilde{V} \cos \omega' t$$

$$I = \left(G_{DC} + \tilde{G} \cos \omega t \right) \left(\tilde{V} \cos \omega' t \right)$$

Mix down to lower freq

$$= G_{DC} \tilde{V} \cos \omega' t + \tilde{G} \tilde{V} \left[\cos(\omega + \omega') t + \cos(\omega - \omega') t \right]$$

monitor the amplitude of $I_{mix}(\omega) = \tilde{G} \tilde{V} \cos(\omega - \omega') t$

while sweeping ω through the mechanical resonance
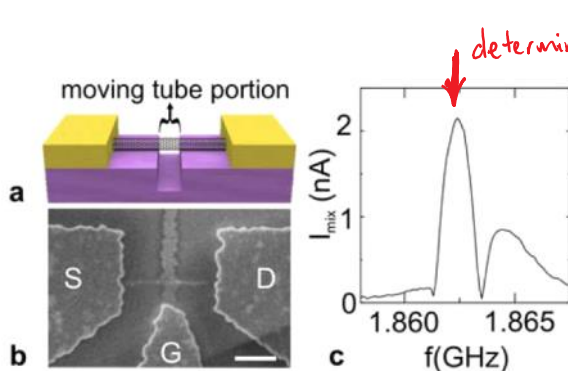
determine mechanical resonance from jump in I_{mix} when CNT motion is large (significant modulation of G)

a moving tube portion

b S   D   G

c
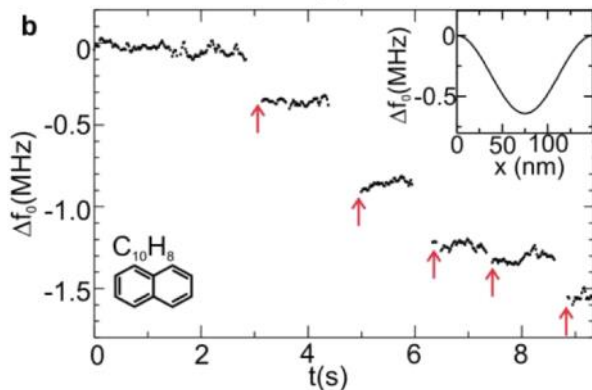
Monitor changes in resonance frequency as single molecules are absorbed.

b

$C_{10}H_8$

Another example using this technique:

Wang et al. "Phase transitions of absorbed atoms" Science (2010).

Surface coverage determined by measuring changes in resonant frequency.

IS 73.7 K
RF?
77.4 K
CS
V
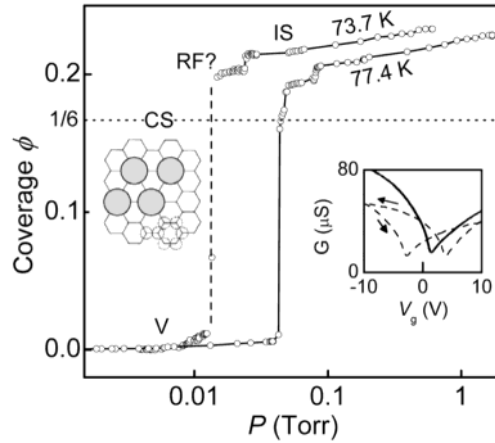
Fig. 3 Adsorption of Kr on device YB3, showing first-order phase transitions. (The 73.7 K isotherm has in-
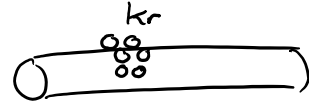
Looking to future... the electronic structure of a material can affect the resonant freq of an oscillator
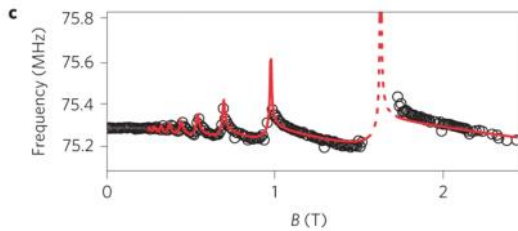
Suspended graphene sheet is resonating at 75 MHz. The filling of Landau levels can be detected in the mechanical resonance.

Chen et al. "Modulation of Mechanical resonance..."
Nature Physics 12 240 (2016)

Mechanical response is a tool to study physics on the surface, and inside the material.

Example 3: Detecting a force gradient (from a nearby charge or magnetic moment)
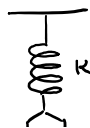
$\downarrow$ smaller F_{ext} $F = -k_{eff} z + \dfrac{dF_{ext}}{} z$

$$F = -K_{eff}\, z + \frac{dF_{ext}}{dz}\, z$$

$$= -\left(K_{eff} - \underbrace{\frac{dF_{ext}}{dz}}\right) z$$

change in the
effective spring const.
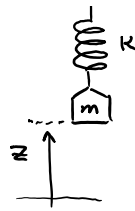
↓ smaller F_{ext}

↓ Bigger F_{ext}

$$\Delta w_i = \frac{\partial w_i}{\partial K_{eff}} \Delta K_{eff}$$

As a charge sensor, or magnetic force sensor,
this mechanical method can outperform other options.

Summary of Part 1

Key parameters of a NEMS system

- $m_{eff,n}$ & $K_{eff,n}$ $\Rightarrow$ w_n ← we often assume that mechanical modes are perfectly decoupled from each other.

- quality factor Q

Need methods to actuate & sense the mechanical motion

- Self-sensing mechanisms — conductance changes ✓ discussed already

  piezo electric   see below

- Modulate the capacitance of an LC circuit.   See below

PART 2:

Measurement & Minipulation of macroscopic resonators
at their quantum limit.

$$k_B T < \hbar w_0 \qquad \text{(a familiar minimum requirement}$$
the level spacing in qubit expts)

10mK

$$w_0 \gtrsim 2\pi \times 1\,GHz$$

Build something stiff and light weight, freq > 1 GHz

cool to 10 mK, measure x_{ZPM}.

First demonstration   O'Connell et al. Nature (2010)

Area 30 μm × 30 μm
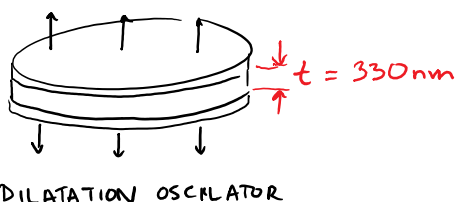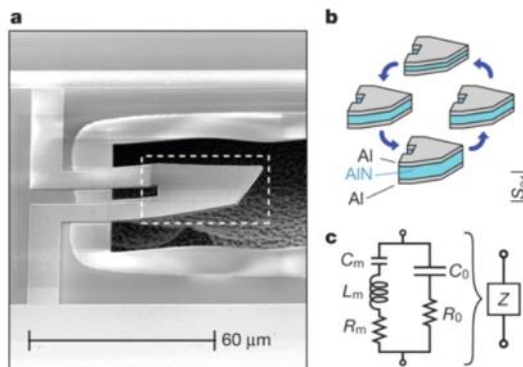
$t = 330$ nm   AlN piezo electric material

DILATATION OSCILLATOR

$$\omega_1 \approx 2\pi \left[6 \text{ GHz} \right] \quad \propto \frac{1}{t}$$

$$m_{eff} \approx 3 \times 10^{-13} \text{ kg}$$

$$Q = 260$$

$$x_{ZPM} = \sqrt{\frac{\hbar}{2m\omega_0}} \approx 6 \times 10^{-17} \text{ m}$$

The tiny piezoelectric voltage was detected by a quantum circuit
(John Martinis group)

The low Q (short mechanical lifetime) prevented
the manipulation of complex mechanical states and direct
tests of entanglement.

A prepared state would last $\sim \dfrac{260}{6 \text{ GHz}} = 40$ ns.

Improved experiments: Teufal et al. Nature (2011)

Drumhead

2 μm

b

ω_d
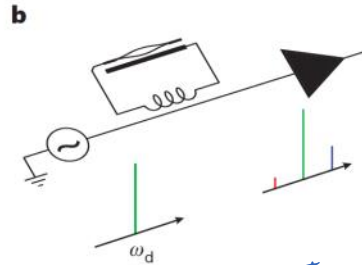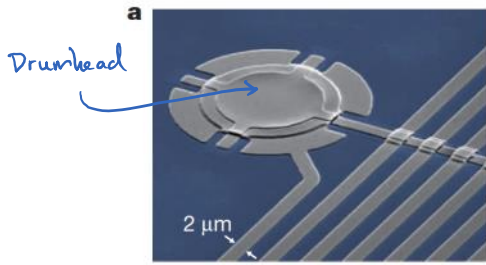
Inductor is
12 nH Spiral inductor

15 μm

$t = 100$ nm

DRUM HEAD
(cross-sectional view)

I'm using a different
symbol to
differentiate
mechanical resonance
from optical resonance.
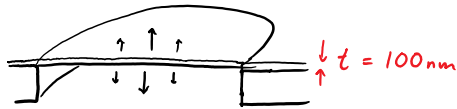
Aluminium membrane

$Q = 300,000$ 1000 times better

$\Omega \approx 2\pi \left[10 \text{ MHz} \right]$ 600 times less

$m_{eff} \approx 4 \times 10^{-14}$ kg   8 times less

$x_{ZPM} = \sqrt{\dfrac{\hbar}{2m\Omega}} \approx 4 \times 10^{-15}$ m   70 times larger

Cannot cool to the ground state by simply loading in a dil fridge.

need a clever trick.

Pump
ω_p

inductively coupled

L

x

$C(x)$
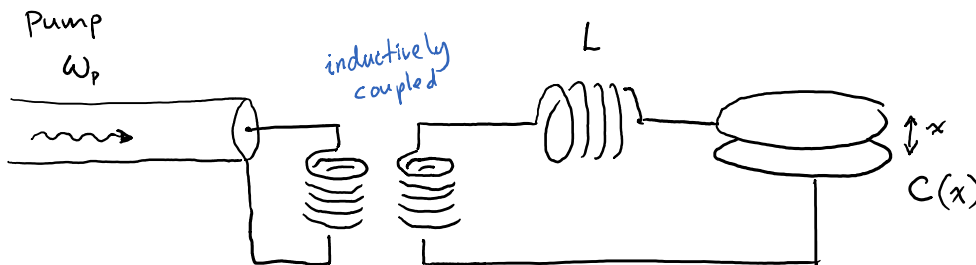
The LC resonator $\equiv$ cavity
(analog to an optical cavity)

$$\omega_{cav}(x) = \frac{1}{\sqrt{LC(x)}}$$

"Parametric coupling" between the cavity and the mechanical resonator

$\underbrace{\qquad}_{\omega_{cav}}$ $\underbrace{\qquad}_{freq\ \Omega}$

For small mechanical vibrations $\omega_{cav}(x) = \omega_{cav} + x \frac{\partial \omega_{cav}}{\partial x} + \ldots$

$$H = \hbar \omega_{cav}(x) a^\dagger a + \hbar \Omega b^\dagger b$$

$$\approx \hbar \omega_{cav} a^\dagger a + \hbar \Omega b^\dagger b + \hbar \hat{x} \frac{\partial \omega_{cav}}{\partial x} a^\dagger a$$

$$\underbrace{\qquad\qquad\qquad} = H_{int}$$

Optomechanic coupling : interaction between "optical system"
& mechanical system

Force on capacitor plate due to radiation pressure

$$F = \frac{dH_{int}}{dx} = \hbar \frac{\partial \omega_{cav}}{\partial x} n_{photons}$$

The optomechanical system starts in a state of n phonons & m photons.

$\underbrace{\qquad}_{\Omega}$ $\underbrace{\qquad}_{\omega_{cav}}$

We drive the system with a "pump" field ω_p

Typically ω_p is chosen to be either $\omega_{cav} + \Omega$ "blue detuning"

ω_{cav}

$\omega_{cav} - \Omega$ "red detuning"

phonon $|n, m\rangle$ photon

$|n-2\; 2\rangle$ $|n-1\; 2\rangle$

$|n-2\; 1\rangle$ $|n-1\; 1\rangle$

$|n-2\; 0\rangle$ $|n-1\; 0\rangle$ $|n, 0\rangle$ $|n+1\; 0\rangle$ $\updownarrow \hbar\Omega$

Energy

$\hbar \omega_{cav}$

destroy phonon,   add photon   cool the mechanical mode
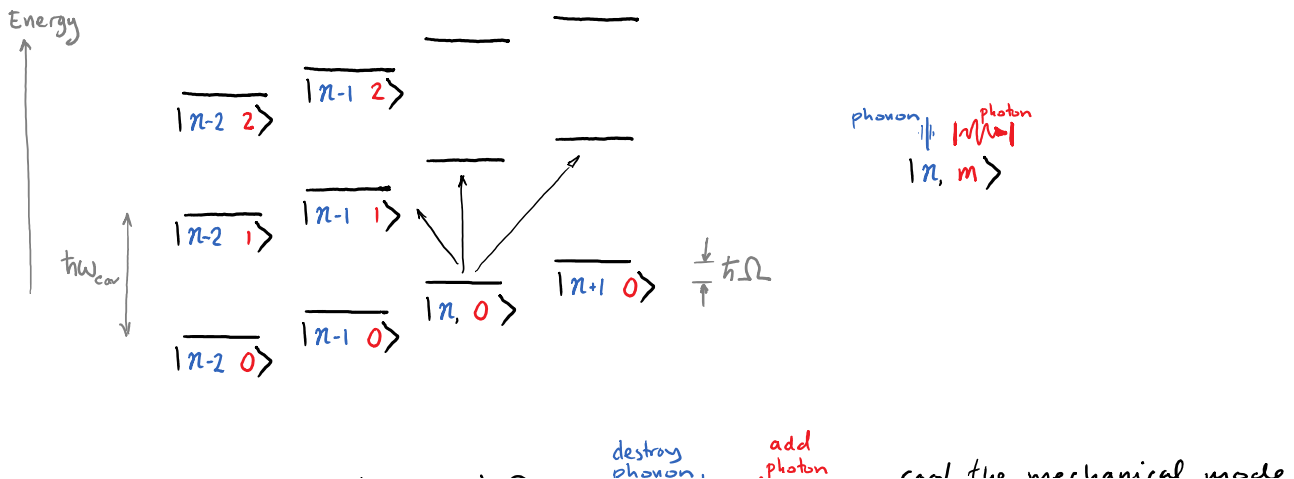
Transitions energy $\quad \hbar \omega_{cav} - \hbar \Omega$ _destroy phonon_ | _add photon_ | cool the mechanical mode

$\hbar \omega_{cav} + \hbar \Omega$ _add phonon_ | _add photon_ | amplify the mechanical mode

(can also say the pump photons has been upconverted/downconverted for cooling /amplifying respectively)

The rate of these cooling /amplifying transitions depends on Magnitude of the Optomechanical coupling:

$$H_{int} = \hbar \hat{x} \frac{\partial \omega_{cav}}{\partial x} a^{\dagger} a$$

position operator for mechanical mode $\quad \hat{x} = x_{ZPF} \left(b^{\dagger} + b \right)$

$$H_{int} = \hbar x_{ZPF} \frac{\partial \omega_{cav}}{\partial x} \left(b^{\dagger} + b \right) a^{\dagger} a = \hbar g_0 \left(b^{\dagger} + b \right) a^{\dagger} a$$

$\Rightarrow$ vacuum optomech coupling rate

$$g_0 = x_{ZPF} \frac{\partial \omega_{cav}}{\partial x}$$

$\Rightarrow$ when there are n_{ph} photons in cavity, optomech coupling rate

$$g = g_0 n_{ph}$$

To analyze the rates in more detail

$\quad \ast \quad$ input - output formalism

account for energy loss rates

Γ for mechanical $\left(Q = \frac{\Omega}{\Gamma} \right)$

κ for optical

* rotating wave approx
  (eliminate fast oscillating terms)

(See page 7-10 of Sorin's notes, attached).

Some key results of calculations

Rate describing removal of energy from the mechanical mode via the optomechanical cooling effect.

$\frac{4g^2}{\kappa} > \Gamma$

κ

$\omega_{cav} - \Omega$ ω_{cav}
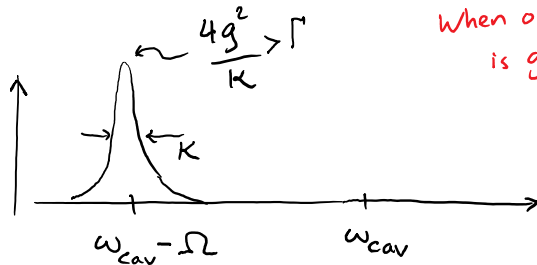
When optical damping rate is greater than mechanical damping $\left(\frac{4g^2}{\kappa} > \Gamma\right)$ then we are effectively cooling the drum. The sideband linewidth depends on κ (energy leaving via the optical cavity)

$\Omega \gg \kappa$

is the resolved sideband limit

Returning to example: Teufel et al. Nature (2011)

15 μm

$t = 100$ nm
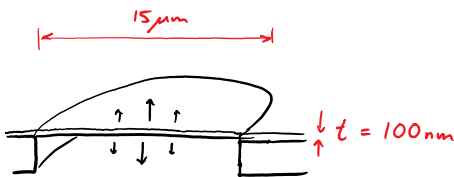
DRUM HEAD
(cross-sectional view)

Aluminium membrane

$\Omega \approx 2\pi \times 10$ MHz

$Q = 300,000$

$\Gamma = 2\pi \times 32$ Hz   (rate that we loose mechanic energy)

$x_{ZPM} = \sqrt{\frac{\hbar}{2m\Omega}} \approx 4 \times 10^{-15}$ m

$\frac{\partial \omega_{cav}}{\partial x} = 2\pi \times 50 \frac{MHz}{nm}$

Optical cavity $\omega_{cav} = 2\pi \times 7.5$ GHz

$Q_{cav} = 30,000$

$\kappa = 2\pi \times 200$ kHz

$\sim \dfrac{4g^2}{\kappa}$

exceeds Γ when $n_{ph} \sim 70$

κ

$\omega_{cav} - \Omega$ ω_{cav}
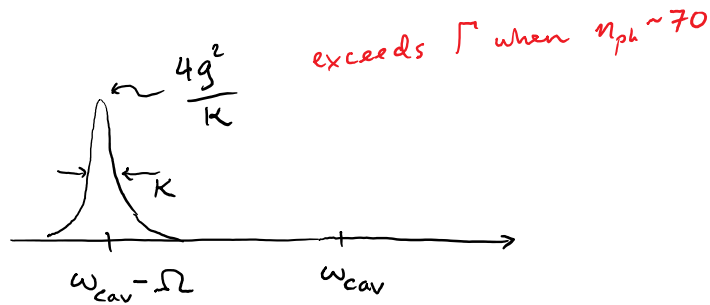
After the drum head is cold (phonon number $n = 0$) it will stay in the prepared state for $\dfrac{1}{\underbrace{n(T=10mK)}_{\text{# of phonons resonator had at 10mK}} \Gamma} \approx 100\,\mu s.$ ← compare to the dilitation oscillator which lasted 40 ns.

To improve these engineered quantum resonators, it is natural to try reducing mass even further.

Prospect of going to atomically thin resonators

15 μm

$t = 0.3\,nm$
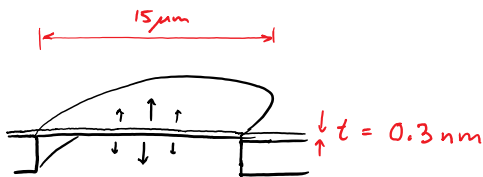
Reduce the mass by factor 300

$X_{ZPM} = \sqrt{\dfrac{\hbar}{2m\Omega}} \approx 80 \times 10^{-15}\,m$ 20 times larger

we can tune Ω by applying tension to the drum head.

Progress has been held back by low Q in resonators made from single layer graphene or carbon nanotubes.

Understanding low Q in atomically thin resonators has taken more than 10 years.

Some recently emerging answers:

- Non-linear mechanics in the Brownian limit.

- Vibrational energy is recurrently shared among several resonance modes.

Barnard et al. "Real-time vibrations of a carbon nanotube"
Nature (2019)
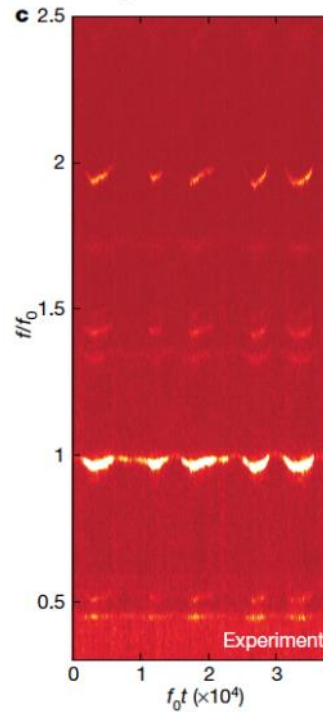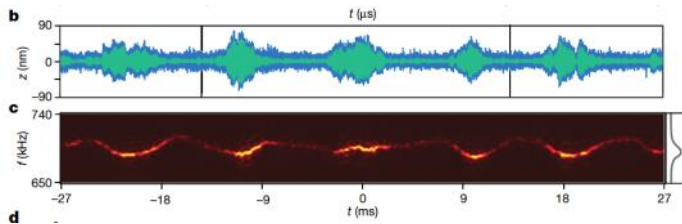
Freq. of mode 1 changes when energy
    is transferred to mode 2.

Complicated non-linearities and coupling.

Ongoing challenge to "tame" these
    atomically thin resonators.

Exciting next steps: Test quantum gravity?

        Chpt 10 of Bowen & Milburn

    massive object in super position of 2 distinct classical states.
    What will happen when test mass flies in-between?

HYPOTHESIS 1: wave fn of massive object collapses and test mass deflected
                left or right.
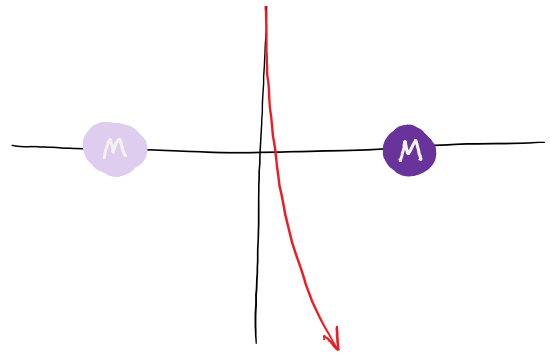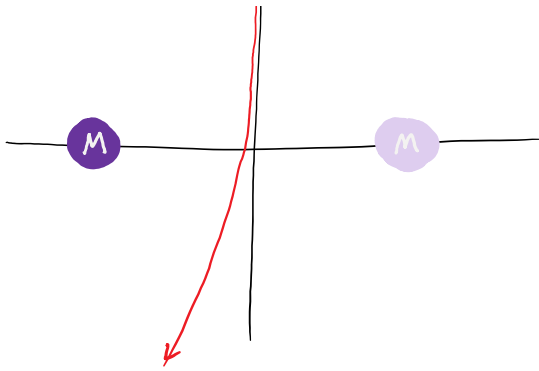
HYPOTHESIS 2: we calculate mass density

$$\rho(\vec{r}) = M|\Psi(\vec{r})|^2 \text{ and predict that the}$$

test mass flies straight through.
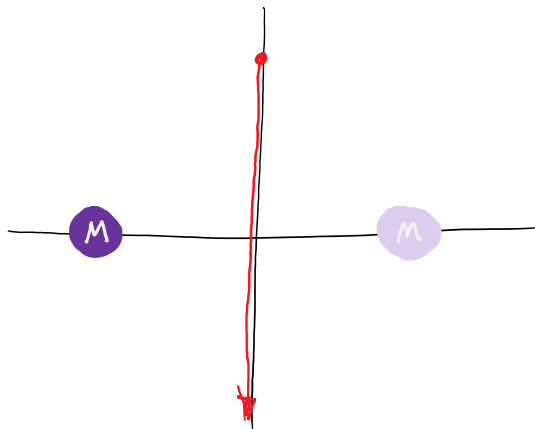
Fundamental question: What is the gravitational field of a massive object that is in 2 distinct classical states?

There are now proposals to test this using drumhead resonators

Nanomechanical systems

G. S. Paraoanu

Low Temperature Laboratory, Department of Applied Physics,

School of Science, Aalto University,

P.O. Box 15100, FI-00076 AALTO,Finland

I. INTRODUCTION

Nanomechanical systems have emerged in recent years as one of the most promising devices where one could witness a variety of quantum mechanical effects. This field has benefited from improvements in nanofabrication and advanced materials, which allowed the fabrication of high-quality mechanical oscillators, as well as from the use of sensitive measurement techniques from nanoelectronics and quantum optics.

In this lecture we will focus on **optomechanical systems**: in these devices a mechanical degree of freedom interacts with a radiation field (either in the microwave or in the optical range) by radiation pressure. The mechanical degree of freedom can be any collective mechanical oscillation (phonon), for example the vibration of a mechanical beam, the oscillations of the surface of a metallic nanoscale drum or that of a suspended sheet of graphene, *etc*. The initial work in this field dates from the years 1970-1980, when people started to develop systems such as laser interferometers and Weber bars for the detection of gravitational waves (tiny ripples in spacetime that would change the distance between mirrors in the interferometers or make the huge cylindrical Weber bars oscillate). Nowadays these devices have reached impressive sensitivities: for example laser interferometers have displacement sensitivities of 10^{-19}m/$\sqrt{\text{Hz}}$, meaning that during a 1 second measurement time they can detect a displacement of 1/1000 radius of a proton [2]. Similarly, the force sensitivity of present-days detectors based on vibrating cantilevers could be improved if these devices could be cooled to remove the thermal noise - which as we will see it is possible in optomechanics. Even now, the sensitivity of atomic force microscopes is of the order of 10^{-18}N/$\sqrt{\text{Hz}}$. This means that in 1 second we can measure the gravitational force between 2 persons, one in New York and the other in Los Angeles [2]. Cooling is one very important process: it would allow us to bring the nanomechanical resonator in a state with only a few quanta of oscillation (phonons) present, therefore applications in the field of quantum information can be foreseen. For typical nanomechanical resonators, the frequency $\Omega_{\text{M}}/2\pi$ is typically 1 MHz - up to a few GHz. Therefore, in order to obtain only a few modes, we would need to cool a 1 MHz resonator to a temperature $T < \hbar\Omega_{\text{M}}/k_{\text{B}}$. A few example of nanomechanical systems are given in Fig. II.
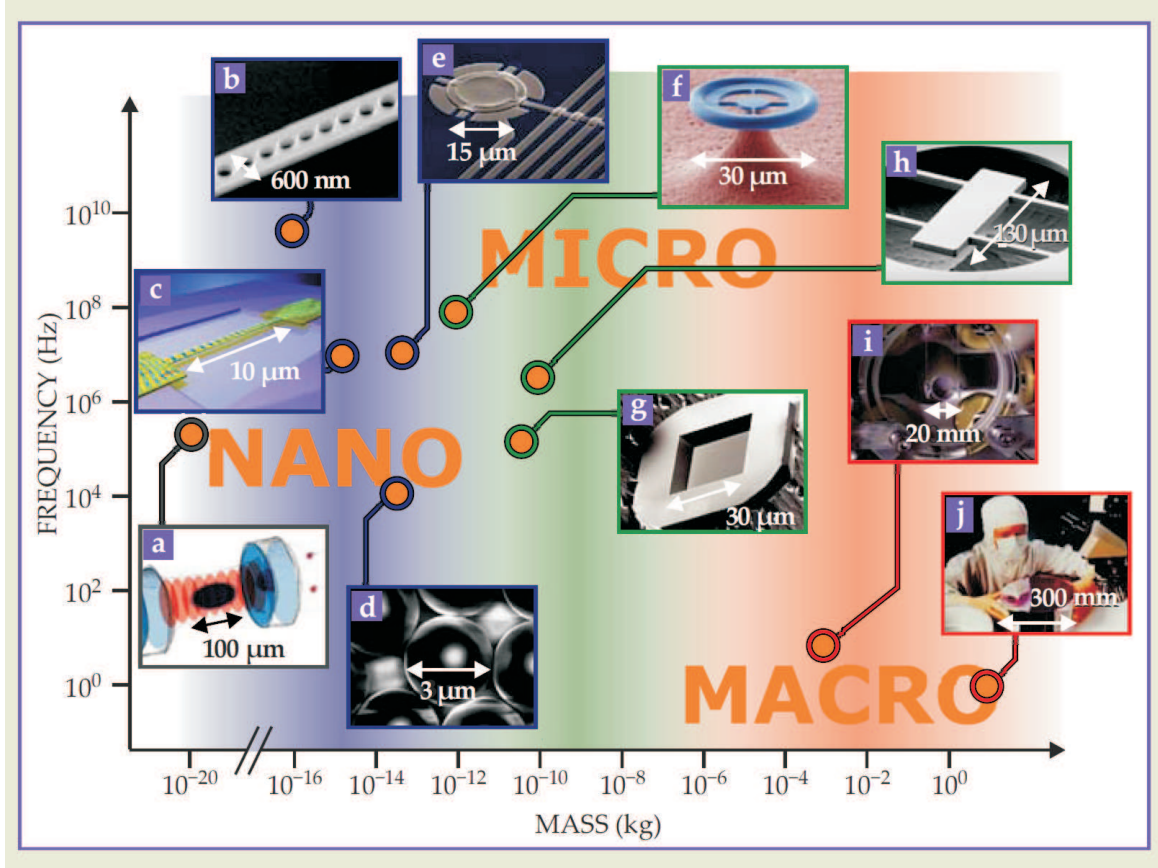
FIG. 1: Nanomechanical systems: (a) ultracold atoms in a cavity (b,c) optical photonic waveguides with mechanical oscillation frequencies (d) microspheres (e) metallic membranes (f) microtoroidal waveguides (g) microscale membranes (h) microscale devices, and (i,j) macroscopic resonators. Figure from Ref. [2].

II. THE STANDARD OPTOMECHANICAL HAMILTONIAN

We consider the generic problem of a nanomechanical resonator that modulates parametrically the frequency of a pumped cavity. Depending on the detuning of the pump with respect to that of the cavity, we define two regimes, corresponding to red-detuned and blue-detuned. In the first regime, we show that the device deamplifies an input signal and cools the nanomechanical resonator; in the second, it functions as a nondegenerate parametric amplifier. There is also a regime called quantum nondemolition regime, defined by a zero value for the detuning, but we will not discuss it further. In Fig. II we present a schematic of these regimes.

3
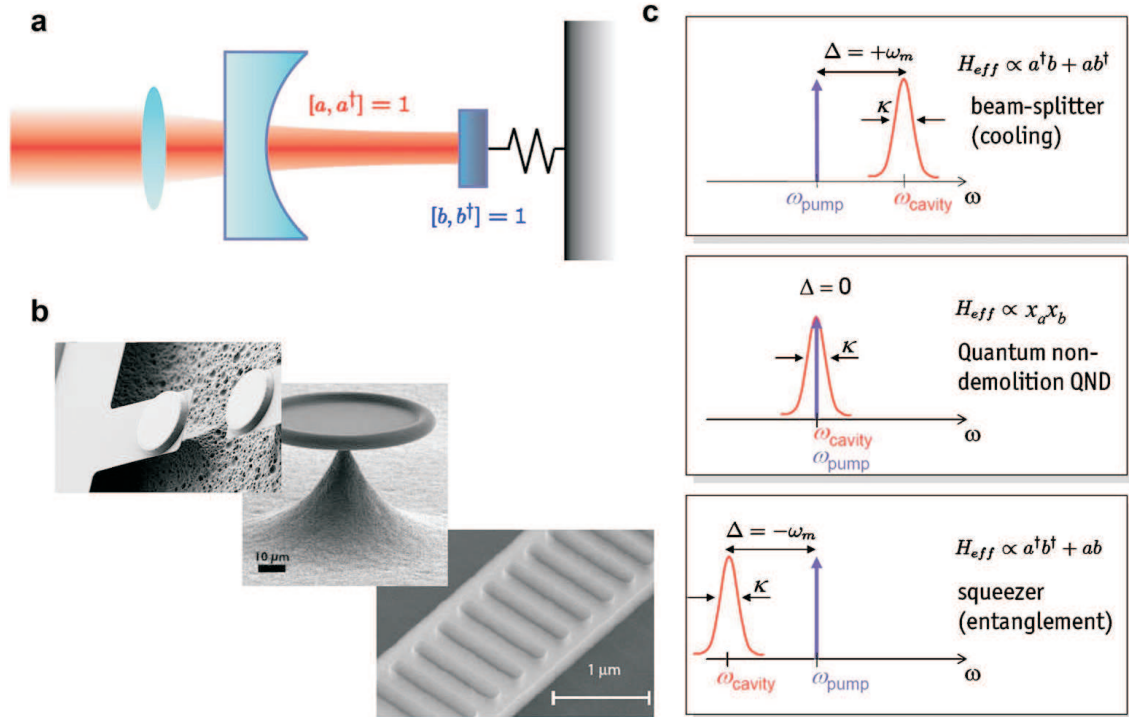
FIG. 2: (a) Standard optomechanical setup consisting of a cavity with a semitransparent mirror (field operators $\hat{a}$, $\hat{a}^\dagger$) coupled to a mechanical resonator (field operators $\hat{b}$, $\hat{b}^\dagger$). (b) Examples: Fabry-Pérot cavity, microtoroidal disc, quasi one-dimensional photonic crystal. (c) Three regimes can be distinguished, depending on the frequency of the pump laser (or microwave) that inputs photons in the cavity: the cooling regime (pump red detuned with respect to the mechanical resonator), quantum nondemolition regime (zero detuning between the pump and the mechanics), and the amplification and squeezing regime (pump is blue-detuned with respect to the mechanical oscillator). Figure from Ref. [1].

A. Interaction Hamiltonian

The first step is to derive the interaction Hamiltonian between the radiation field in the cavity and the mechanical mode. We will consider a single optical or microwave mode a, $a^\dagger$, confined in a cavity with resonance frequency ω_{cav}. We assume that the cavity frequency depends on the displacement of a mechanical oscillator b, $b^\dagger$ with frequency Ω_{M}, for example if this oscillator serves as a mirror it will change the optical length (therefore the frequency) of the cavity as it vibrates,

$$\omega_{\text{cav}}(x) \approx \omega_{\text{cav}} + x\frac{\partial\omega_{\text{cav}}}{\partial x} + \ldots \tag{1}$$

4

Let us define the optical frequency shift per displacement as

$$G = \frac{\partial \omega_{\text{cav}}}{\partial x}. \tag{2}$$

Thus for this system we have

$$H = \hbar \omega_{\text{cav}}(x) a^\dagger a + \hbar \Omega_{\text{M}} b^\dagger b \tag{3}$$

$$\approx \hbar \omega_{\text{cav}} a^\dagger a + \hbar \Omega_{\text{M}} b^\dagger b + H_{\text{int}}, \tag{4}$$

where

$$H_{\text{int}} = G x a^\dagger a = \hbar g_0 a^\dagger a (b + b^\dagger). \tag{5}$$

Here $x = x_{\text{ZPF}}(b^\dagger + b)$, and x_{ZPF} represents the value of zero-point fluctuations in position of the nanomechanical device,

$$x_{\text{ZPF}} = \sqrt{\frac{\hbar}{2m\Omega_{\text{M}}}}, \tag{6}$$

and g_0 is called the optomechanical single-photon coupling strength,

$$g_0 = x_{\text{ZPF}}(\partial \omega_{\text{cav}} / \partial x) = G x_{\text{ZPF}}. \tag{7}$$

The Hamiltonian then reads

$$H = \hbar \Omega_{\text{M}} \left(b^\dagger b + \frac{1}{2} \right) + \hbar (\omega_{\text{cav}} + g_0 z) \left(a^\dagger a + \frac{1}{2} \right), \tag{8}$$

where to remind about notations, Ω_{M} is the resonance frequency of the nanomechanical device, ω_{cav} is the cavity resonance frequency, and $z = x/x_{\text{ZPF}} = b^\dagger + b$.

From H_{int} we can immediately find the force due to radiation pressure,

$$F = \frac{dH_{\text{int}}}{dx} = \hbar G a^\dagger a = \hbar \frac{g_0}{x_{\text{ZPF}}} a^\dagger a. \tag{9}$$

In the input-output formalism, the field equations for the cavity mode a (with decay rate κ) and the mechanical mode b (with decay rate Γ_{M}) read

$$\dot{a} = -i(\omega_{\text{cav}} + g_0 z)a - \frac{\kappa}{2}a - \sqrt{\kappa} a_{\text{in}}, \tag{10}$$

$$\dot{b} = -i\Omega_M b - i g_0 \left(a^\dagger a + \frac{1}{2} \right) - \frac{\Gamma_{\text{M}}}{2} b - \sqrt{\Gamma_{\text{M}}} b_{\text{in}}, \tag{11}$$

This type of Hamiltonian is obtained in both optical and microwave setups, see Fig. II A.
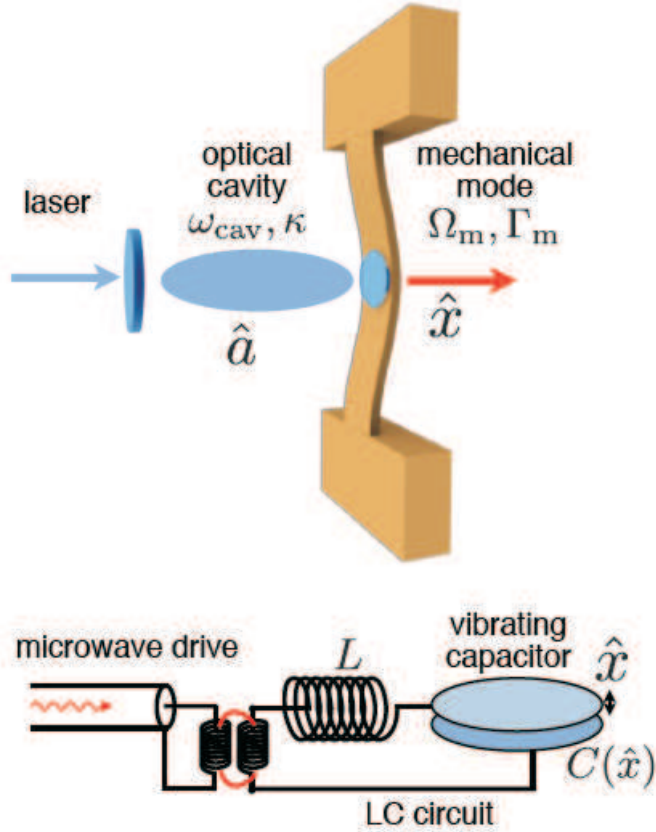
FIG. 3: Generic optical and microwave setups leading to the Hamiltonian Eq. (8). Figure from Ref. [3].

B. Scales

It is useful to give a few numbers before proceeding further. The mechanical frequency Ω_{M} can be from kHz to GHz, the effective masses m of the oscillators can be $m \approx 10^{-15} - 10^{-3}\mathrm{kg}$, leading to x_{ZPF} typically of the order of $10^{-15}\mathrm{m}$. This is an incredibly small displacement (of the same order as the radius of the proton), that, surprisingly, can be measured very accurately in rather small-scale optomechanical setups that fit in a normal lab. The optomechanical single-photon couling g_0 is of the order of 100 Hz to a few MHz (in photonic crystals). κ can be from MHz to GHz, Γ_{M} from Hz to MHz, and the mechanical quality factor $Q_{\mathrm{M}} = \Omega_{\mathrm{M}}/\Gamma_M = 10^5 - 10^7$.

C. Driven cavity

The cavity is pumped at a frequency ω_L, therefore we can separate the pump

$$a_{\text{in}}(t) = \exp(-i\omega_L t)[\bar{a}_{\text{in}} + d_{\text{in}}(t)], \tag{12}$$

and search for a solution for the cavity field in the form

$$a(t) = \exp(-i\omega_L t)[\bar{a} + d(t)], \tag{13}$$

$$b(t) = \bar{b} + c(t), \tag{14}$$

where $\bar{a}$ and $\bar{b}$ are time-independent (stationary) classical fields. Note that $\bar{b}_{in} = 0$, in other words on the mechanical side we assume that the system admits in only fluctuations (as typically coming from a thermal bath). Using these expressions in Eq. (10,11) we find for the stationary fields

$$\bar{a} = -\sqrt{\kappa}(\kappa/2 - i\Delta)^{-1}\bar{a}_{\text{in}}, \tag{15}$$

$$\bar{b} = -i\frac{g_0}{\Gamma_{\text{M}}/2 + i\Omega_{\text{M}}}\left(|\bar{a}|^2 + \frac{1}{2}\right), \tag{16}$$

with $\Delta = \omega_L - \omega_{\text{cav}} - g_0\bar{z}$, where

$$\bar{z} = \bar{b} + \bar{b}^* = -\frac{2g_0\Omega_{\text{M}}}{(\Gamma_{\text{M}}/2)^2 + \Omega_{\text{M}}^2}\left(|\bar{a}|^2 + \frac{1}{2}\right) \tag{17}$$

is the stationary displacement of the position of the nanomechanical beam due to radiation pressure. Note that typically the nanomechanical frequency is about three to six orders of magnitude larger than Γ_{M}, thus to a very good approximation $\bar{z} \approx -2(g_0/\Omega_{\text{M}})\left(|\bar{a}|^2 + \frac{1}{2}\right)$.

To find the equations for $d(t)$ and $c(t)$, we linearize the Heisenberg equations around the pump field, and obtain a system of coupled equations describing the dynamics of the nanomechanical and electromagnetic degrees of freedom,

$$\dot{d} = i\Delta d - \frac{\kappa}{2}d - \sqrt{\kappa}d_{\text{in}} + i\alpha(c + c^\dagger), \tag{18}$$

$$\dot{c} = -i\Omega_{\text{M}}c - \frac{\Gamma_{\text{M}}}{2}c - \sqrt{\Gamma_{\text{M}}}c_{\text{in}} + i(\alpha^* d + \alpha d^\dagger), \tag{19}$$

where $\alpha = -g_0\bar{a}$. One often encounters the notation $g = |\alpha| = g_0\sqrt{<a^\dagger a>} = g_0\sqrt{\bar{n}_{\text{cav}}}$, which is called **light-enhanced optomechanical coupling**. This system can be solved by Fourier transform. We will use systematically throughout this paper the convention

7

from [4], for the Fourier transform of the adjoint of an operator, that is $c^\dagger(\omega) = [c(-\omega)]^\dagger$, $d^\dagger(\omega) = [d(-\omega)]^\dagger$. Also, we introduce the standard notations for the bare mechanical susceptibility, $\chi_M(\omega) = [\Gamma_M/2 - i(\omega - \Omega_M)]^{-1}$ and for the resonator (cavity) susceptibility $\chi_{cav}(\omega) = [k/2 - i(\omega + \Delta)]^{-1}$. To see the structure of Eqs. (18,19) it is useful to regard the mechanical and electromagnetic degrees of freedom as two-component fields defined by

$$\check{c}(\omega) = \begin{bmatrix} c(\omega) \\ c^\dagger(\omega) \end{bmatrix} ; \quad \check{d}(\omega) = \begin{bmatrix} d(\omega) \\ d^\dagger(\omega) \end{bmatrix}, \tag{20}$$

and introduce the matrices of the bare mechanical (M) and resonator (R) susceptibilities, as well as the coupling matrices A and $\tilde{A}$,

$$M(\omega) = \begin{bmatrix} \chi_M^{-1}(\omega) & 0 \\ 0 & \chi_M^{-1}(-\omega)^* \end{bmatrix} ; \tag{21}$$

$$R(\omega) = \begin{bmatrix} \chi_{cav}^{-1}(\omega) & 0 \\ 0 & \chi_{cav}^{-1}(-\omega)^* \end{bmatrix} ; \tag{22}$$

$$A = \begin{bmatrix} -i\alpha^* & -i\alpha \\ i\alpha^* & i\alpha \end{bmatrix} ; \quad \tilde{A} = \begin{bmatrix} -i\alpha & -i\alpha \\ i\alpha^* & i\alpha^* \end{bmatrix}. \tag{23}$$

The structure of Eq. (23) is therefore quite transparent: it shows that the fields $\check{c}$ and $\check{d}$ are coupled to each other by the off-diagonal matrices A and $\tilde{A}$. In the absence of this coupling, the fields C and D would evolve independently and, moreover, the components c, $c^\dagger$ and d, $d^\dagger$ would be decoupled since the susceptibility matrices M and R are diagonal.

With these notations, Eqs. (18,19) can be put in the form

$$\begin{bmatrix} M(\omega) & A \\ \tilde{A} & R(\omega) \end{bmatrix} \begin{bmatrix} \check{c}(\omega) \\ \check{d}(\omega) \end{bmatrix} = - \begin{bmatrix} \sqrt{\Gamma_M}\check{c}_{in}(\omega) \\ \sqrt{k}\check{d}_{in}(\omega) \end{bmatrix}. \tag{24}$$

The system Eq. (24) can be solved by inverting the 4×4 matrix on the left hand side. The determinant of this matrix is $\chi_{cav}^{-1}(\omega)\chi_{cav}^{-1}(-\omega)^*\mathcal{N}(\omega)$, where $\mathcal{N}(\omega) = \chi_M^{-1}(\omega)\chi_M^{-1}(-\omega)^* + 2\Omega_M\Sigma(\omega)$, where $\Sigma(\omega) = -i|\alpha|^2[\chi_{cav}(\omega) - \chi_{cav}(-\omega)^*]$ is called **resonator self-energy**. Two important properties of these quantities, which are useful to simplify the form of the equations, can be readily checked out, namely $\Sigma(\omega) = [\Sigma(-\omega)]^*$ and $\mathcal{N}(\omega) = [\mathcal{N}(-\omega)]^*$.

The result for the fields $\check{c}(\omega)$ and $\check{d}(\omega)$ can be written as

$$\check{c}(\omega) = -\frac{\sqrt{\Gamma_M}}{\mathcal{N}(\omega)}S(\omega)\check{c}_{in}(\omega) - \frac{\sqrt{k}}{\mathcal{N}(\omega)}T(\omega)\check{d}_{in}(\omega), \tag{25}$$

$$\breve{d}(\omega) = -\frac{\sqrt{k}}{\mathcal{N}(\omega)}V(\omega)\breve{d}_{\text{in}}(\omega) - \frac{\sqrt{\Gamma_{\text{M}}}}{\mathcal{N}(\omega)}W(\omega)\breve{c}_{\text{in}}(\omega), \tag{26}$$

and for the elements of the 2×2 matrices S, T, V, W we have the results

$$S_{11}(\omega) = S_{22}(-\omega)^* = \chi_{\text{M}}^{-1}(-\omega)^* - i\Sigma(\omega); \tag{27}$$

$$S_{12}(\omega) = S_{21}(-\omega)^* = -i\Sigma(\omega); \tag{28}$$

$$T_{11}(\omega) = T_{22}(-\omega)^* = i\alpha^*\chi_{\text{M}}^{-1}(-\omega)^*\chi_{\text{cav}}(\omega); \tag{29}$$

$$T_{12}(\omega) = T_{21}(-\omega)^* = i\alpha\chi_{\text{M}}^{-1}(-\omega)^*\chi_{\text{cav}}(-\omega)^*; \tag{30}$$

$$W_{11}(\omega) = W_{22}(-\omega)^* = i\alpha\chi_{\text{M}}^{-1}(\omega)\chi_{\text{cav}}(\omega); \tag{31}$$

$$W_{12}(\omega) = W_{21}(-\omega)^* = i\alpha\chi_{\text{M}}^{-1}(-\omega)^*\chi_{\text{cav}}(\omega); \tag{32}$$

$$V_{11}(\omega) = V_{22}(-\omega)^* = [\chi_{\text{M}}^{-1}(-\omega)^*\chi_{\text{M}}^{-1}(\omega) + 2i\Omega_{\text{M}}|\alpha|^2\chi_{\text{cav}}(-\omega)^*]\chi_{\text{cav}}(\omega); \tag{33}$$

$$V_{12}(\omega) = V_{21}(-\omega)^* = -2i\Omega_{\text{M}}\alpha^2\chi_{\text{cav}}(-\omega)^*\chi_{\text{cav}}(\omega). \tag{34}$$

Now, using these equations all the correlation functions can be evaluated for any value of the parameters entering the problem. Physically however there are only three relevant choices, corresponding to zero detuning of the pump field and to $\Delta = \pm\Omega_{\text{M}}$.

- **The cooling regime** Cooling and deamplification of a signal occurs for $\Delta = -\Omega_{\text{M}}$, or $\omega_{\text{L}} = \omega_{\text{cav}} - \Omega_{\text{M}}$ (laser red-detuned by the mechanical resonance frequency with respect to the cavity). The frequency $\omega_{\text{cav}} - \Omega_{\text{M}}$ is also called Stokes sideband.

- **Amplification and squeezing regime** Amplification and squeezing occur for $\Delta = \Omega_{\text{M}}$, or $\omega_{\text{L}} = \omega_{\text{cav}} + \Omega_{\text{M}}$ (laser blue-detuned by the mechanical resonance frequency with respect to the cavity). The frequency $\omega_{\text{cav}} + \Omega_{\text{M}}$ is also called anti-Stokes sideband.

- **The quantum nondemolition regime** The $\Delta = 0$ regime (laser on resonance with the cavity) is relevant for performing nondemolition measurements on the nanomechanical resonator.

Compared to other equations obtained in the literature in various approximations (depending on the concrete experimental setup) the expressions presented above have the advantage that they are exact and yet simple enough to be used for comparison with experimental results. Moreover, they are universal, in the sense that they do not depend on the specific experimental setup: they can be used equally well for optical and microwave systems.

parameter	mechanical resonator	cavity
frequency	Ω_{M}	ω_{cav}
decay rate	Γ_{M}	κ
susceptibility	$\chi_{\mathrm{M}}(\omega) = [\Gamma_{\mathrm{M}}/2 - i(\omega - \Omega_{\mathrm{M}})]^{-1}$	$\chi_{\mathrm{cav}}(\omega) = [\kappa/2 - i(\omega + \Delta)]^{-1}$
detuning		$\Delta = \omega_L - \omega_{\mathrm{cav}}$

TABLE I: Notations used for the nanomechanical resonator and the cavity. Here ω_L is the "laser" (pump) frequency.

III.   THE RESOLVED-SIDEBAND LIMIT

Given that the general solutions Eqs. (27-34) are obtained, using them for any particular experimental setup is straightforward. A natural classification of these setups is with respect to the pumping and probe-beam frequencies: we then have optical-frequencies and microwave-frequencies experiment. Yet in Eq. (10, 11) only the mechanical frequency and the detuning with respect to the pump (which is of the same order of magnitude as the mechanical frequency) appear. From this point of view there is no difference between mechanical and optical setups. What makes however a difference is the quality factor of the cavity used: for

$$\kappa/\Omega_{\mathrm{M}} \ll 1 \tag{35}$$

we are in the resolved sideband regime; otherwise not. Some existing experiments are in this regime or somewhat close (for example, for one experiment at NIST the reported values are $\Omega_{\mathrm{M}} = 2\pi \times 10.69$ MHz, $\kappa = 2\pi \times 170$ kHz, $\kappa/\Omega_{\mathrm{M}} = 0.016$, putting it into the deep resolved sideband regime, the Vienna group [5] has $\kappa = 2\pi \times 215$ kHz, $\Omega_M = 2\pi \times 947$ kHz, $\kappa/\Omega_{\mathrm{M}} = 0.2$ and for the experiments at LTL $\Omega_M = 2\pi \times 32$ MHz, $\kappa = 2\pi \times 10$MHz, $\kappa/\Omega_{\mathrm{M}} = 0.31$), while others are definitely not (for example another experiment at NIST [7] has $\Omega_M = 2\pi \times 1.04$ MHz, $\kappa = 2\pi \times 2.88$MHz, $\kappa/\Omega_{\mathrm{M}} = 2.77$).

Here we show that in sideband resolved regime it is possible to get a very clear picture of the physics behind cooling and especially amplification. Although one could get directly our results by simply performing the relevant approximation in the equations above, it is more satisfying to start with the general equations and show that the solutions in the resolved sideband cooling limit can be obtained by performing a second rotating wave approximation.

10

Indeed, by writing the Hamiltonian Eq. (8) in the rotating frame at the pumping frequency ω_L and expanding it around the stationary states Eqs. (15,16) we find

$$H = H_{\text{eff}} - \hbar\Delta(\bar{a}d^\dagger + \bar{a}^*d) + \hbar g_0|\bar{a}|^2(c + c^\dagger), \tag{36}$$

where

$$H_{\text{eff}} = \hbar\Omega_{\text{M}}c^\dagger c - \hbar\Delta d^\dagger d + \hbar g_0(c + c^\dagger)(\bar{a}^*d + \bar{a}d^\dagger) \tag{37}$$

One recognizes here the expression of a system described by the Hamiltonian H_{eff}, which comprises two oscillators, described by the operators d and c, both driven by the coherent field $\{\bar{a}, \bar{a}^*\}$, but with different types of field-oscillator coupling.

The Liouville equations $\partial_t(\bar{a} + d) = \frac{i}{\hbar}[H, \bar{a} + d] - \frac{\kappa}{2}(\bar{a} + d) - \sqrt{\kappa}(\bar{a}_{\text{in}} + d_{\text{in}})$ and $\partial_t(\bar{b} + c) = \frac{i}{\hbar}[H, \bar{b} + c] - \frac{\Gamma_{\text{M}}}{2}(\bar{b} + c) - \sqrt{\Gamma_{\text{M}}}c_{\text{in}}$ are equivalent to $\dot{d} = \frac{i}{\hbar}[H_{\text{eff}}, d] - \frac{\kappa}{2}d - \sqrt{\kappa}d_{\text{in}}$ and $\dot{c} = \frac{i}{\hbar}[H, c] - \frac{\Gamma_{\text{M}}}{2}c - \sqrt{\Gamma_{\text{M}}}c_{\text{in}}$, and, in turn, to Eqs. (18,19) after using Eqs. (15,16), namely $\bar{a} = -\sqrt{\kappa}/(\kappa/2 - i\Delta)^{-1}\bar{a}_{\text{in}}$, $\bar{b} = -i\frac{g_0}{\Gamma_{\text{M}}/2+i\Omega_{\text{M}}}\left(|\bar{a}|^2 + \frac{1}{2}\right)$ and the fact that $\bar{a}$ and $\bar{b}$ are time-independent. Thus the system is described by $H_{\text{eff}} = \hbar\Omega_{\text{M}}c^\dagger c - \hbar\Delta d^\dagger d - \hbar(c + c^\dagger)(\alpha^*d + \alpha d^\dagger)$ and its associated Liouville equations. We now notice that in a rotating frame defined by the transformation $U(t) = \exp[i\hbar(\Omega_{\text{M}}c^\dagger c - \Delta d^\dagger d)t]$ the Hamiltonian H_{eff} transforms as $\tilde{H}_{\text{eff}} = U(t)H_{\text{eff}}U^\dagger(t) + \left[i\hbar\frac{\partial}{\partial t}U(t)\right]U^\dagger(t)$, and eliminate the time-dependent (rotating) terms.

- **Cooling regime** When $\Delta = -\Omega_{\text{M}}$ (red-detuning) the remaining terms in the Hamiltonian are

$$\tilde{H}_{\text{eff}}^{(\text{RWA})} = -\hbar(\alpha^*c^\dagger d + \alpha d^\dagger c), \tag{38}$$

or, going back to the original frame,

$$H_{\text{eff}}^{(\text{RWA})} = \hbar\Omega_{\text{M}}\left(c^\dagger c + d^\dagger d\right) - \hbar(\alpha^*c^\dagger d + \alpha d^\dagger c). \tag{39}$$

The Hamiltonians Eqs. (38,39) describe two coupled harmonic oscillators. The coupling term has the form of the **beam-splitter** interaction in optics: in a beam splitter, a photon coming from a mode b corresponding to one input direction can exit into the mode c (another direction) or the other way around. The same procedure can be applied directly in the Heisenberg picture. Take $d(t) = e^{i\Delta t}\tilde{d}(t)$ and $c(t) = e^{-i\Omega_{\text{M}}t}\tilde{c}(t)$ and insert them into Eq. (18,19); by neglecting the counter-rotating terms we obtain in the "cooling" regime

$$\dot{\tilde{d}} = i\alpha\tilde{c} - \frac{k}{2}\tilde{d} - \sqrt{k}\tilde{d}_{\text{in}}; \tag{40}$$

$$\dot{\tilde{c}} = i\alpha^*\tilde{d} - \frac{\Gamma_{\text{M}}}{2}\tilde{c} - \sqrt{\Gamma_{\text{M}}}\tilde{c}_{\text{in}}. \tag{41}$$

- **Amplification regime** When $\Delta = +\Omega_{\text{M}}$ (blue-detuning), the remaining terms of the Hamiltonian are

$$\tilde{H}_{\text{eff}}^{(\text{RWA})} = -\hbar(\alpha^*cd + \alpha d^\dagger c^\dagger), \tag{42}$$

or, going back to the original frame,

$$H_{\text{eff}}^{(\text{RWA})} = \hbar\Omega_{\text{M}}\left(c^\dagger c - d^\dagger d\right) - \hbar(\alpha^*cd + \alpha d^\dagger c^\dagger). \tag{43}$$

In this case Eqs. (42,43) correspond to a **two-mode squeezing** interaction between the modes b and c, which lead to amplification. Note also that one of the oscillators becomes inverted, thus matching nicely a well-known model of amplification from quantum optics. The same procedure can be applied directly in the Heisenberg picture. Take $d(t) = e^{i\Delta t}\tilde{d}(t)$ and $c(t) = e^{-i\Omega_{\text{M}}t}\tilde{c}(t)$ and insert them into Eq. (18,19); by neglecting the counter-rotating terms we get in the "amplification" regime

$$\dot{\tilde{d}} = i\alpha\tilde{c}^\dagger - \frac{k}{2}\tilde{d} - \sqrt{k}\tilde{d}_{\text{in}}; \tag{44}$$

$$\dot{\tilde{c}}^\dagger = -i\alpha^*\tilde{d} - \frac{\Gamma_{\text{M}}}{2}\tilde{c}^\dagger - \sqrt{\Gamma_{\text{M}}}\tilde{c}_{\text{in}}^\dagger. \tag{45}$$

- **The nondemolition regime**

  In this case $\Delta = 0$ and from Eq. (37) we immediately obtain

$$H_{\text{eff}} = \hbar\Omega_{\text{M}}c^\dagger c - \hbar\frac{2g_0\bar{a}_{\text{in}}}{\sqrt{k}}(c + c^\dagger)(d + d^\dagger), \tag{46}$$

where we have used $\bar{a} = -2\bar{a}_{\text{in}}/\sqrt{\kappa}$ at the cavity resonance $\omega_{\text{L}} = \omega_{\text{cav}}$. This is called nondemolition regime due to the resemblance of the interaction part $(c + c^\dagger)(d + d^\dagger)$ with non-demolition Hamiltonians used in quantum optics for non-demolition measurements. Non-demolition measurements of observables are realized by using Hamiltonian interactions that commute with the observables. Suppose that we are interested in the observable $d + d^\dagger$, we can see that it commutes with H_{eff}: this means that once we measure it, the Hamiltonian evolution will not affect it anymore and if we measure it again we will find the same value. Also, using this interaction Hamiltonian, the mechanical displacement $x_{\text{ZPF}}(c + c^\dagger)$ can be read out through the phase shift of the laser field entering the cavity.

Note that in Fourier space going from c to $\tilde{c}$ amounts to translations in frequency, namely for an arbitrary frequency ω, $\tilde{d}(\omega) = d(\omega - \Delta)$, $\tilde{d}^\dagger(\omega) = d^\dagger(\omega + \Delta)$, $\tilde{c}(\omega) = c(\omega + \Omega_M)$, $\tilde{c}^\dagger(\omega) = c^\dagger(\omega - \Omega_M)$. Clearly, Eqs. (40, 41) and Eqs. (44, 45) are the Liouville equations corresponding to $\tilde{H}_{\text{eff}}^{\text{(RWA)}} = -\hbar(\alpha^* c^\dagger d + \alpha d^\dagger c)$ and $\tilde{H}_{\text{eff}}^{\text{(RWA)}} = -\hbar(\alpha^* cd + \alpha d^\dagger c^\dagger)$ respectively.

A.   The cooling regime

A schematic of the transitions in the cooling regime (laser red-detuned) is shown in Fig. 4. When the cavity is placed at the frequency $\omega_L + \Omega_M$, scattering occurs preferentially along the "blue" arrows, and the photons emitted from the cavity carry the energy $\hbar\omega_L + \hbar\Omega_M$, that is, a phonon $\hbar\Omega_M$ is absorbed from the mechanical resonator and its energy is found in the output laser beam.
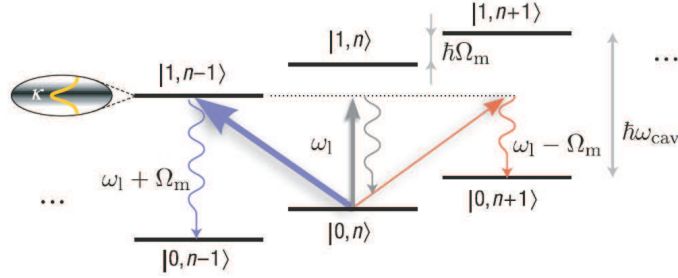

FIG. 4: Diagram of transitions. The cavity, if it is higher in frequency than the laser, enhances the transitions that result in loss of phonons from the mechanical resonator. Figure from Ref. [3].

From Eqs. (40,41), going to the Fourier transform and then going back to the initial c, d by using the frequency-translation relations we find

$$\begin{bmatrix} \chi_M^{-1}(\omega) & -i\alpha^* \\ -i\alpha & \chi_{\text{cav}}^{-1}(\omega) \end{bmatrix} \begin{bmatrix} c(\omega) \\ d(\omega) \end{bmatrix} = \begin{bmatrix} -\sqrt{\Gamma_M} c_{\text{in}}(\omega) \\ -\sqrt{k} d_{\text{in}}(\omega) \end{bmatrix} \tag{47}$$

This equation can be obtained from the more general form Eq. (24) by projecting on the relevant subspace identified by the rotating-wave approximation described above.

The solution of this equation is

$$c(\omega) = -\frac{1}{\chi_M^{-1}(\omega)\chi_{\text{cav}}^{-1}(\omega) + |\alpha|^2} \left[\sqrt{\Gamma_M} \chi_{\text{cav}}^{-1}(\omega) c_{\text{in}} + i\alpha^* \sqrt{k} d_{\text{in}}(\omega) \right], \tag{48}$$

$$d(\omega) = -\frac{1}{\chi_M^{-1}(\omega)\chi_{\text{cav}}^{-1}(\omega) + |\alpha|^2} \left[i\alpha \sqrt{\Gamma_M} c_{\text{in}}(\omega) + \chi_M^{-1}(\omega) \sqrt{k} d_{\text{in}}(\omega) \right], \tag{49}$$

13

Validity of the rotating wave approximation

It is useful to remind ourselves here that $\Delta = -\Omega_M$ and a typical measurement would monitor the noise within a few mechanical linewidths Γ_M around Ω_M, *i.e.* $\omega = \Omega_M + \delta$, and therefore $\chi_M^{-1}(\omega) = \Gamma_M/2 - i\delta$, $\chi_{cav}^{-1}(\omega) = \kappa/2 - i\delta$. Since δ is of the same order of magnitude as Γ_M and $\Gamma_M \ll \Omega_M$ it follows that $\chi_M^{-1}(-\omega) \approx 2i\Omega_M$, $\chi_{cav}^{-1}(-\omega) \approx 2i\Omega_M$, $\Sigma(\omega) \approx -i|\alpha|^2\chi_{cav}(\omega)$, $\mathcal{N}(\omega) \approx -2i\Omega_M\chi_{cav}(\omega)[\chi_{cav}^{-1}(\omega)\chi_M^{-1}(\omega) + |\alpha|^2]$. Using these approximations, we can verify that the solutions Eqs. (48, 49) can be obtained from Eqs. (25, 26) and Eqs. (27-34) provided that $|\alpha| \ll \sqrt{\Gamma_M\Omega_M}$. This condition is satisfied well enough for the typical range of powers used in the experiments.

Generalized Manley-Rowe relations for the cooling regime

The classical Manley-Rowe relations for the cooling regime show that in the absence of dissipation, the sum of the number of photons generated per unit time in the cavity and in the mechanical resonator is zero. This reflects the fact that every time that a photon is produced, a phonon in the resonator must be absorbed and the other way around. A generalized quantum-mechanical version of these relations in the presence of dissipation can be obtained from Eqs. (40,41). Since photons and phonons are lost through the cavity and the fixing points of the mechanical resonator at rates k respectively Γ_M, we should add these leaked photons when accounting for the particles that the Hamiltonian is generating, and define $\dot{n}_d = \partial_t(d^\dagger d) + kd^\dagger d$ and $\dot{n}_c = \partial_t(c^\dagger c) + \Gamma_M c^\dagger c$. Then, from Eqs. (40,41) we obtain

$$\dot{n}_d + \dot{n}_c = -\sqrt{k}(d_{in}^\dagger d + d^\dagger d_{in}) - \sqrt{\Gamma_M}(c_{in}^\dagger c + c^\dagger c_{in}). \tag{50}$$

The classical Manley-Rowe relation reads $\dot{n}_d + \dot{n}_c = 0$. What Eq. (50) shows is that, in the presence of dissipation, even if we would attempt to account for particle losses through the classical rates $\kappa d^\dagger(t)d(t)$ and $\Gamma_M c^\dagger(t)c(t)$, there are still correlations between the input fields and the cavity and resonator operators that have to be considered, as evident from the right hand side of Eq. (50).

An useful and perhaps more transparent way to look at Eqs. (38,39) is to take $\omega = \Omega_M + \delta$, $\delta \ll \Omega_M$. Then we have:

$$c(\omega) = -\frac{1}{(\Gamma_M/2 - i\delta)(\kappa/2 - i\delta) + |\alpha|^2}[\sqrt{\Gamma_M}(k/2 - i\delta)c_{in}(\delta) + i\alpha^*\sqrt{\kappa}d_{in}(\delta)]; \tag{51}$$

$$d(\omega) = -\frac{1}{(\Gamma_M/2 - i\delta)(k/2 - i\delta) + |\alpha|^2}[i\alpha\sqrt{\Gamma_M}c_{in}(\delta) + (\sqrt{\Gamma_M}/2 - i\delta)\sqrt{\kappa}d_{in}(\delta)]; \tag{52}$$

$$c^\dagger(\omega) = 0; \tag{53}$$

14

$$d^\dagger(\omega) = 0, \tag{54}$$

from which $c(-\omega)$, $d(-\omega)$, $c^\dagger(-\omega)$, and $d^\dagger(-\omega)$ can be derived by the use of $c(-\omega) = [c^\dagger(\omega)]^\dagger$, $c^\dagger(-\omega) = [c(\omega)]^\dagger$, *etc.*.

We now can calculate a number of relevant correlations. For correlations the following notation is useful, $\langle \mathcal{A}(\omega)\mathcal{B}(-\omega')\rangle = \langle \mathcal{AB}\rangle(\omega)\delta(\omega - \omega')$, where $\mathcal{A}$, $\mathcal{B}$ are two arbitrary operators. We then have

Self-correlations

One important quantity in the case of cooling is the number of phonons in the micromechanical resonator at a given frequency; this quantity is nonzero around the cavity frequency,

$$\langle c^\dagger c\rangle(-\omega) = \frac{1}{|(\Gamma_{\rm M}/2 - i\delta)(\kappa/2 - i\delta) + |\alpha|^2|^2} \left[(\kappa/2 + \delta^2)\Gamma_{\rm M}\langle c^\dagger_{\rm in} c_{\rm in}\rangle(-\omega) + |\alpha|^2\kappa\langle d^\dagger_{\rm in} d_{\rm in}\rangle(-\omega) \right]. \tag{55}$$

Cross-correlations

$$\langle cd^\dagger\rangle(\delta) = \frac{1}{|(\Gamma_{\rm M}/2 - i\delta)(\kappa/2 - i\delta)| + |\alpha|^2|^2} \left[i\alpha^*\Gamma_{\rm M}(k/2 - i\delta)\langle c_{\rm in} c^\dagger_{\rm in}\rangle(\delta) + i\alpha^*\kappa(\Gamma_{\rm M}/2 + i\delta)\langle d_{\rm in} d^\dagger_{\rm in}\rangle(\delta) \right]. \tag{56}$$

This shows that even when the system is fed uncorrelated noise, it will generate, by its own dynamics, correlations between the nanomechanical resonator and the cavity. This happens even if the input states are mechanical and electromagnetic vacuum. We also note that due to this correlations the nanomechanical resonator and the cavity can be regarded as forming a qubit. Indeed, using the Schwinger representation, we have $\sigma_z = d^\dagger d - c^\dagger c$, $\sigma_x = \sigma_+ + \sigma_- = d^\dagger c + c^\dagger d$, and $\sigma_y = -i(\sigma_+ + \sigma_-) = -i(d^\dagger c - c^\dagger d)$, and therefore $H_{eff}^{\rm (RWA)} = \hbar\Omega_{\rm M}I - \hbar(\alpha\sigma_+ + \alpha^*\sigma_-)$. One recognizes here the interaction-picture Hamiltonian of a two-level system x- and y- coupled to a classical field $\{\alpha, \alpha^*\}$.

B. The amplification regime

This time, if we look in Fig. 4, the cavity will be placed in the $|1, n+1 >$ state, and the laser is at $\omega_{\rm L} = \omega_{\rm cav} + \Omega_{\rm M}$. Note that the Hamiltonians Eqs. (42,43) allows indeed the coupling of states $|0, n >$ with $|1, n+1 >$ (indeed, terms that create or annihilate simultaneously a photon and a phonon are present in this Hamiltonians). Thus a signal $d_{\rm in}$

can be amplified by using the energy of the laser beam. This is somewhat similar to what happens in a laser, where the pump is used to create a population inversion.

In the same way as before, from Eqs. (44,45), going to the Fourier transform and then going back to the initial c, d by using the frequency-translation relations we find

$$
\begin{bmatrix} \chi_M^{-1}(-\omega)^* & i\alpha^* \\ -i\alpha & \chi_{\text{cav}}^{-1}(\omega) \end{bmatrix} \begin{bmatrix} c^\dagger(\omega) \\ d(\omega) \end{bmatrix} = \begin{bmatrix} -\sqrt{\Gamma_M} c_{\text{in}}^\dagger(\omega) \\ -\sqrt{k} d_{\text{in}}(\omega) \end{bmatrix} \tag{57}
$$

Again, we can verify that this equation can be obtained from the more general form Eq. (24) by projecting on the relevant subspace identified by the rotating-wave approximation described above.

The solution of this equation is

$$
c^\dagger(\omega) = -\frac{1}{\chi_M^{-1}(-\omega)^* \chi_{\text{cav}}^{-1}(\omega) - |\alpha|^2} \left[\sqrt{\Gamma_M} \chi_{\text{cav}}^{-1}(\omega) c_{\text{in}}^\dagger - i\alpha^* \sqrt{\kappa} d_{\text{in}}(\omega) \right], \tag{58}
$$

$$
d(\omega) = -\frac{1}{\chi_M^{-1}(-\omega)^* \chi_{\text{cav}}^{-1}(\omega) - |\alpha|^2} \left[i\alpha \sqrt{\Gamma_M} c_{\text{in}}^\dagger(\omega) + \chi_M^{-1}(-\omega)^* \sqrt{\kappa} d_{\text{in}}(\omega) \right]. \tag{59}
$$

Validity of the rotating wave approximation

Again, we analyze here the validity of the rotating wave approximation in the amplification regime. This time, $\Delta = \Omega_M$ and with the notation $\omega = -\Omega_M + \delta$ we have $\chi_M^{-1}(-\omega) = \Gamma_M/2 + i\delta$, $\chi_{\text{cav}}^{-1}(-\omega) = \kappa/2 + i\delta$, $\chi_M^{-1}(\omega) \approx 2i\Omega_M$, $\chi_{\text{cav}}^{-1}(-\omega) \approx -2i\Omega_M$, $\Sigma(\omega) \approx -i|\alpha|^2 \chi_{\text{cav}}(\omega)$, $\mathcal{N}(\omega) \approx 2i\Omega_M \chi_{\text{cav}}(\omega)[\chi_M^{-1}(\omega)^* \chi_{\text{cav}}^{-1}(\omega) - |\alpha|^2]$. Again, only for values of δ not much higher than Γ_M we can get some nonzero values for the fields. We can again verify that the solutions Eqs. (44, 45) can be obtained from Eqs. (25, 26) and Eqs. (27-34) provided that $|\alpha| \ll \sqrt{\Gamma_M \Omega_M}$.

Generalized Manley-Rowe relations for the amplification regime

In the amplification regime, the classical Manley-Rowe relations show that the rates of photon production and phonon production are the same. This reflects the fact that photons and phonons are born in this system at the same time. The quantum Manley-Rowe relations for the amplification regime can be again obtained from Eqs. (44,45),

$$
\dot{n}_d - \dot{n}_c = -\sqrt{\kappa}(d_{\text{in}}^\dagger d + d^\dagger d_{\text{in}}) + \sqrt{\Gamma_M}(c_{\text{in}}^\dagger c + c^\dagger c_{\text{in}}). \tag{60}
$$

Again we encounter a quantum-mechanical phenomenon, namely that once you open the system to the external world it is not sufficient to account classically for the particles lost

16

through the definitions $\dot{n}_d = \partial_t(d^\dagger d) + \kappa d^\dagger d$ and $\dot{n}_c = \partial_t(c^\dagger c) + \Gamma_{\mathrm{M}} c^\dagger c$, but there will be correlations being built between the field in the cavity and resonator and the input fields.

It is also useful to write explicitly the frequency components given by Eqs. (58,59) around the cavity resonance, that is $\omega = -\Omega_{\mathrm{M}} + \delta$, $\delta \ll \Omega_{\mathrm{M}}$,

$$c^\dagger(\omega) = -\frac{1}{(\Gamma_{\mathrm{M}}/2 - i\delta)(\kappa/2 - i\delta) - |\alpha|^2}[\sqrt{\Gamma_{\mathrm{M}}}(\kappa/2 - i\delta)c_{\mathrm{in}}^\dagger(\delta) - i\alpha^* \sqrt{\kappa} d_{\mathrm{in}}(\delta)]; \qquad (61)$$

$$d(\omega) = -\frac{1}{(\Gamma_{\mathrm{M}}/2 - i\delta)(\kappa/2 - i\delta) - |\alpha|^2}[i\alpha \sqrt{\Gamma_{\mathrm{M}}}c_{\mathrm{in}}^\dagger(\delta) + (\sqrt{\Gamma_{\mathrm{M}}}/2 - i\delta)\sqrt{\kappa} d_{\mathrm{in}}(\delta)]; \quad (62)$$

$$c(\omega) = 0; \qquad (63)$$

$$d^\dagger(\omega) = 0. \qquad (64)$$

from which $d(-\omega)$, $d^\dagger(-\omega)$, $c^\dagger(-\omega)$, $c^\dagger(-\omega)$, and can be derived by the use of $d(-\omega) = [d^\dagger(\omega)]^\dagger$, $d^\dagger(-\omega) = [d(\omega)]^\dagger$, $etc..$

IV. SUMMARY

We have discussed the two most important regimes for optomechanical systems, cooling and amplification. A systematic diagram of these processes is presented in Fig. 5.

---

[1] M. Aspelmeyer, S. Gröblacher, K. Hammerer, and N. Kiesel JOSA B, Vol. 27, Issue 6, pp. A189-A197 (2010); in: JOSA B Feature Issue on Quantum Optical Information Technologies, P. Grangier, A. Jordan, G. Morigi (Eds.)

[2] M. Aspelmeyer. P. Meystre, K.Schwab, Physics Today 65 (7), 29 (2012).

[3] M. Aspelmeyer, T. J. Kippenberg, and F. Marquardt, arXiv:1303.0733.

[4] A. A. Clerk, M. H. Devoret, S. M. Girvin, F. Marquardt, R. J. Schoelkopf, Rev. Mod. Phys. **82**, 1155 (2010).

[5] S. Gröblacher, K. Hammerer, M. R. Vanner, and M. Aspelmeyer, Nature **460**, 724 (2009).

[6] J. D. Teufel, D. Li, M. S. Allman, K. Cicak, A. J. Sirois, J. D. Whittaker, R. W. Simmonds, Nature **471**, 204 (2011).

[7] J. D. Teufel, T. Donner, M. A. Castellanos-Beltran, J. W. Harlow, K. W. Lehnert, Nature Nanotechnology **4**, 820 (2009).
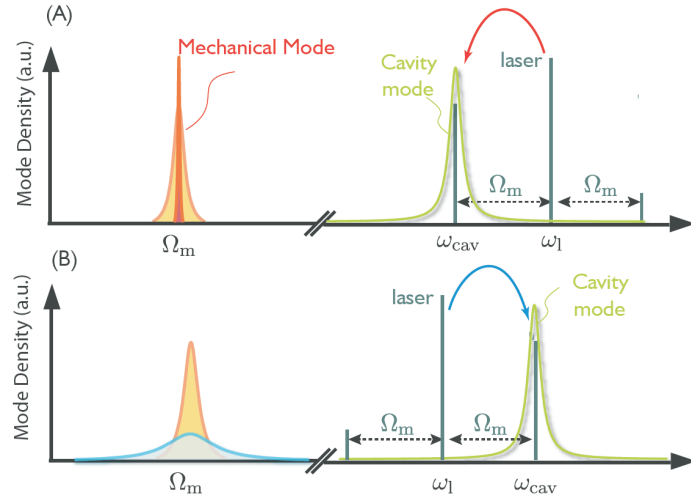
FIG. 5: (A) Amplification (laser is blue-detuned with respect to the cavity) and (B) cooling (laser is red-detuned with respect to the cavity). Scattering from the laser into the cavity is enhanced, leading to the amplification (suppressing of the anti-Stokes process and enhancing the Stokes process) and cooling (suppressing the Stokes processes and enhancing the anti-Stokes processes). Figure from Ref.[3].